

# Probing Lorentz invariance and other fundamental symmetries in ${}^3\text{He}/{}^{129}\text{Xe}$ clock-comparison experiments

M Burghoff<sup>1</sup>, C Gemmel<sup>2</sup>, W Heil<sup>2,4</sup>, S Karpuk<sup>2</sup>, W Kilian<sup>1</sup>, S Knappe-Grüneberg<sup>1</sup>, K Lenz<sup>2</sup>, W Müller<sup>1</sup>, K Tullney<sup>2</sup>, U Schmidt<sup>3</sup>, A Schnabel<sup>1</sup>, F Seifert<sup>1</sup>, Yu Sobolev<sup>2</sup>, and L Trahms<sup>1</sup>

<sup>1</sup>*Physikalisch-Technische Bundesanstalt, Berlin 10587, Germany*

<sup>2</sup>*Institut für Physik, Johannes-Gutenberg Universität, Mainz 55099, Germany*

<sup>3</sup>*Physikalisches Institut, Universität Heidelberg, Heidelberg 69120, Germany*

E-mail: [wheel@uni-mainz.de](mailto:wheel@uni-mainz.de)

**Abstract:** We discuss the design and performance of a very sensitive low-field magnetometer based on the detection of free spin precession of gaseous, nuclear polarized  ${}^3\text{He}$  or  ${}^{129}\text{Xe}$  samples with a SQUID as magnetic flux detector. Characteristic spin precession times  $T_2^*$  of up to 60 h were measured in low magnetic fields (about  $1\text{ }\mu\text{T}$ ) and in the regime of motional narrowing. With the detection of the free precession of co-located  ${}^3\text{He}/{}^{129}\text{Xe}$  nuclear spins (clock comparison), the device can be used as ultra-sensitive probe for non-magnetic spin interactions, since the magnetic dipole interaction (Zeeman-term) drops out in the weighted frequency difference, i.e.,  $\Delta\omega = \omega_{\text{He}} - \gamma_{\text{He}}/\gamma_{\text{Xe}} \cdot \omega_{\text{Xe}}$ . We report on searches for a) Lorentz violating signatures by monitoring the Larmor frequencies of co-located  ${}^3\text{He}/{}^{129}\text{Xe}$  spin samples as the laboratory reference frame rotates with respect to distant stars (sidereal modulation) and b) spin-dependent short-range interactions induced by light, pseudoscalar bosons such as the axion invented to solve the strong CP problem.

## 1. Introduction

${}^3\text{He}/{}^{129}\text{Xe}$  clock comparison experiments based on free spin precession can be used as ultra-sensitive probe for non-magnetic spin interactions of type

$$V_{\text{non-magn}} = \vec{a} \cdot \vec{\sigma} \equiv -\vec{\mu}_{\text{PM}} \cdot \vec{B}_{\text{PM}} \quad (1)$$

The most precise tests of new physics are often realized in differential experiments that compare the transition frequencies of two co-located clocks, typically radiating on their Zeeman or hyperfine transitions. An essential assumption in this so-called clock comparison experiments is that the anomalous field  $\vec{a}$  does not couple to magnetic moments but directly to the sample spins  $\vec{\sigma}$ . This direct coupling allows co-magnetometry that uses two different spin species to distinguish between a normal magnetic field and an anomalous field coupling. The advantage of differential measurements is that they render the experiment insensitive to common systematic effects, such as uniform magnetic field fluctuations. That's why clock comparison experiments are often used to study fundamental symmetries of nature, such as

a) looking for Lorentz-violating signatures by monitoring, e.g., the relative Larmor frequencies or phases of the co-located  ${}^3\text{He}$  and  ${}^{129}\text{Xe}$  spin samples as the laboratory reference frame rotates with respect to distant stars [1]:

$$V(r)/\hbar = \langle \tilde{b} \rangle \hat{\varepsilon} \cdot \vec{\sigma} / \hbar, \quad (2)$$

b) in searches for spin-dependent short-range interactions induced by light, pseudoscalar bosons (CP-violation) [2]:

<sup>4</sup>corresponding author

$$V(r)/\hbar = c\vec{\sigma} \cdot \hat{r}/\hbar, \quad (3)$$

as well as

c) in searches for the electric dipole moment of  $^{129}\text{Xe}$  (CP-violation) [3]:

$$V(r)/\hbar = -|d_{\text{Xe}}| \vec{\sigma} \cdot \vec{E}/\hbar. \quad (4)$$

The observable to trace possible tiny non-magnetic spin interactions is the combination of measured Larmor frequencies given by

$$\Delta\omega = \omega_{L,\text{He}} - \frac{\gamma_{\text{He}}}{\gamma_{\text{Xe}}} \cdot \omega_{L,\text{Xe}} \quad (5)$$

By that measure, the Zeeman-term is eliminated and thus any dependence on fluctuations and drifts of the magnetic field.  $\Delta\omega$  or its equivalent, the residual phase  $\Delta\Phi(t) = \Phi_{\text{He}}(t) - \gamma_{\text{He}}/\gamma_{\text{Xe}} \cdot \Phi_{\text{Xe}}(t)$ , is the relevant quantity to be further analyzed in order to trace tiny symmetry violations of the type as mentioned above.

The essential difference, in particular to the  $^3\text{He}/^{129}\text{Xe}$  spin masers used so far, is, that by monitoring the free spin precession, an ultra-high sensitivity can be achieved with a clock which is almost completely decoupled from the environment. The design and operation of the two-species  $^3\text{He}/^{129}\text{Xe}$  co-magnetometer has been shown recently [4].

## 2. Concept of long nuclear-spin phase coherence times and measurement sensitivity of a $^3\text{He}/^{129}\text{Xe}$ clock based on free spin precession

The magnetometer is based on the detection of free spin-precession of gaseous, nuclear spin-polarized  $^3\text{He}$  or  $^{129}\text{Xe}$  samples. Like in standard NMR, the free induction decay of the transverse magnetization is monitored and the Larmor frequency  $f$  of the precessing sample magnetization is related to the magnetic field  $B_0$  through

$$f = \gamma/(2\pi) \cdot B_0, \quad (6)$$

where  $\gamma$  is the gyromagnetic ratio of the corresponding nucleus. Since this type of magnetometer will preferably operate at low magnetic fields and thus at low frequencies, using a SQUID as magnetic field detector is appropriate due to its high sensitivity in that spectral range. The  $^3\text{He}/^{129}\text{Xe}$  nuclear spins are polarized by means of optical pumping. Thus, the nuclear polarization obtained exceeds the Boltzmann polarization in typical NMR experiments by four to five orders of magnitude. The overall sensitivity of our  $^3\text{He}/^{129}\text{Xe}$ -SQUID co-magnetometer can be estimated using the statistical signal processing theory [5]: for a given sampling rate  $r_s$  with  $r_s/2 \geq f$ , the recorded signal  $S$  from the precessing spins can be written as:

$$S[n] = A \cdot \cos(2\pi \cdot (f/r_s) \cdot n + \Phi) + w[n] \quad n = 0, 1, 2, 3, \dots, N-1 \quad (7)$$

where  $\Phi$  is the initial phase,  $A$  the signal amplitude, and  $T = N/r_s$  the observation time. If the noise  $w[n]$  is Gaussian distributed, the Cramer-Rao Lower Bound (CRLB) sets the lower limit on the variance  $\sigma_f^2$  for the frequency estimation.

$$\sigma_f^2 \geq \frac{12}{(2\pi)^2 \cdot (\text{SNR})^2 \cdot f_{\text{BW}} \cdot T^3} \cdot C(T_2^*) \quad (8)$$

with  $SNR$  being the signal-to-noise ratio.  $C(T_2^*)$  describes the effect of exponential damping of the signal amplitude with  $T_2^*$ . For observation times  $T \leq T_2^*$ ,  $C(T_2^*)$  is of order one. Deviations from the CRLB power law, due to noise sources inherent in the co-magnetometer itself did not show up in Allan standard deviation plots used to identify the power-law model for the phase noise spectrum of our runs with  $T \approx 14$  h, typically [4].

For a  $SNR$  of 10000:1 in a bandwidth of  $f_{BW} = 1$  Hz and an observation time  $T$  of  $T=14$  h, the frequency can be measured with an accuracy of

$$\sqrt{\sigma_f^2} \approx 5 \text{ pHz.} \quad (9)$$

One major technical development was the increase of the storage times of nuclear spin polarized noble gases in low-relaxation glass vessels. The results are published in [6-8]. Then it is possible to preserve spin polarization well over 100 hours. The long  $T_1$  relaxation times (longitudinal relaxation time) are the prerequisite to obtain long transverse relaxation times  $T_2^*$ , too. In standard NMR experiments, typical  $T_2^*$  relaxation times (free induction decay followed by an RF-pulse) are of order ms, only. However, at low magnetic fields ( $\sim 1 \mu\text{T}$ ) and at low gas pressures ( $\sim \text{mbar}$ ), i.e., in the regime of motional narrowing,  $T_2^*$ -times can reach hours or days. Based on the Redfield theory of relaxation due to randomly fluctuating magnetic fields, analytical expressions can be derived for the transverse relaxation rate for spherical and cylindrical sample cells, as reported in [9] and [10], respectively. The general expression for the transverse relaxation rate  $1/T_2^*$  for a spherical sample cell of radius  $R$  is [9]

$$\frac{1}{T_2^*} = \frac{1}{T_1} + \frac{4R^4\gamma^2}{175D} \left( \left| \vec{\nabla}B_{1,y} \right|^2 + \left| \vec{\nabla}B_{1,z} \right|^2 + 2\left| \vec{\nabla}B_{1,x} \right|^2 \right) \quad (10)$$

For long  $T_1$ -times ( $T_1 > 100$ h), the loss of phase coherence of the atoms mainly is due to the fluctuating magnetic field seen by the atoms as they diffuse through the cell (self diffusion). In the regime of motional narrowing the field gradient induced rate then gets proportional to the square of the absolute field gradients, the fourth power of the cell radius  $R$ , and to  $1/D \sim p$ , i.e., proportional to the gas pressure  $p$ .

The "magnetically best shielded room on Earth" is located on the site of the Physikalisch-Technische Bundesanstalt (PTB), Institute Berlin. Magnetic fields such as that of the Earth are kept out here as effective as nowhere else. The instrumental setup at the PTB in Berlin consists of a SQUID vector magnetometer system, which was originally designed for biomagnetic applications inside the strongly magnetically shielded room BMSR-2 ( $(2.9 \times 2.9 \times 2.9) \text{ m}^3$ ) [11]. It consists of 304 DC-SQUID magnetometers divided up into 19 identical modules which are housed in a Dewar. The residual magnetic field gradients are of order  $\text{pT/cm}$ . The sample cells are placed directly below the Dewar as close as possible to a low- $T_c$  SQUID sensor, which detects a sinusoidal  $B$  field change due to the spin precession of the gas atoms (see figure 1).

The operating conditions summarized:

- i) Inside BMSR-2, the white system noise is  $\approx 2.3 \text{ fT}/\sqrt{\text{Hz}}$ , only.
- ii) The recorded signal  $S$  from the precessing spins results in a measured signal-to-noise ratio ( $SNR$ ) of  $SNR > 5000:1$  in a bandwidth of 1 Hz (see figure 1)
- iii) From the exponential decay of the signal amplitude ( ${}^3\text{He}$ ) a transverse relaxation time of  $T_{2,\text{He}}^* \approx 60$  h could be deduced. Meanwhile, the nuclear spin phase coherence time could be increased to  $T_2^* = 100$  h.
- iv)  ${}^{129}\text{Xe}$  is polarized by spin-exchange optical pumping [12] using the existing setup at PTB, whereas  ${}^3\text{He}$  is polarized at Mainz by metastability exchange optical pumping [13] and transported in relaxation free storage vessels to Berlin.
- v) The  ${}^{129}\text{Xe}$  spin coherence time, at present, is limited to  $4 \text{ h} \leq T_2^* \leq 6 \text{ h}$  due to wall relaxation  $T_{1,\text{wall}}^{Xe}$ . The relatively short  $T_{1,\text{wall}}^{Xe}$  relaxation time of  ${}^{129}\text{Xe}$  ( $6 \text{ h} < T_{1,\text{wall}}^{Xe} < 10 \text{ h}$ ) limits the total observation time  $T$  of free spin-precession in our  ${}^3\text{He}/{}^{129}\text{Xe}$  clock comparison experiments. Efforts to increase

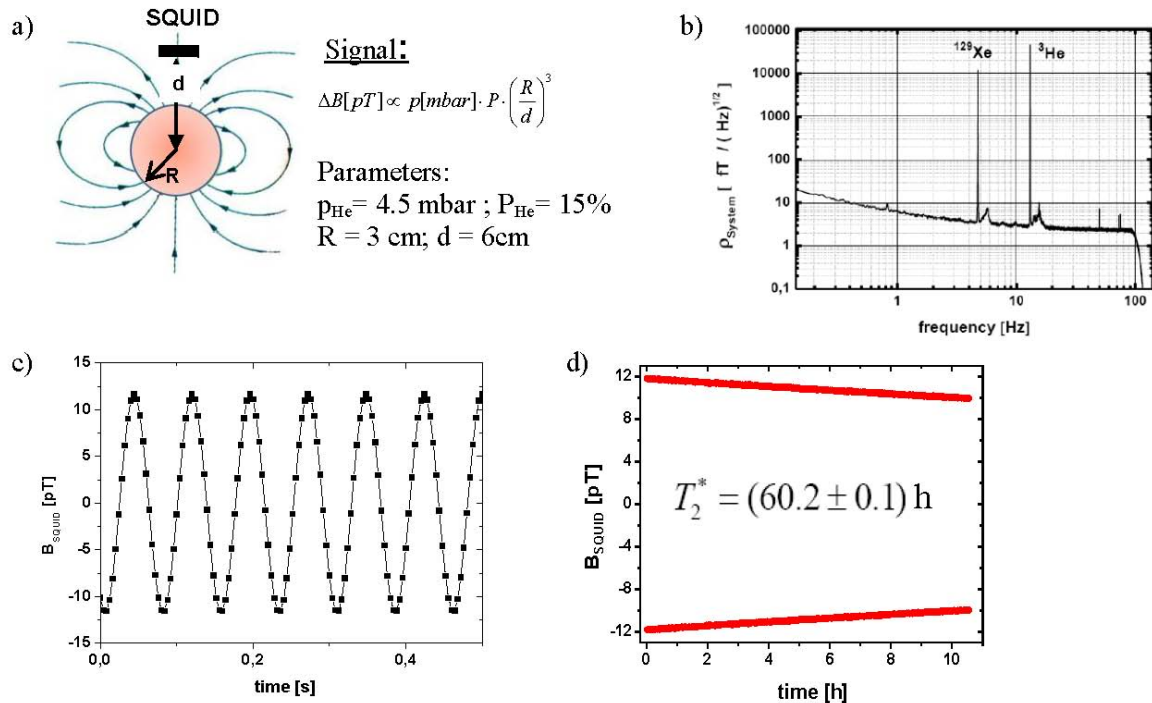


Figure 1: **a)** Signal estimate for spherical sample cell. **b)** Magnetic flux density spectrum of a SQUID that measures the precession of  $^3\text{He}$  and  $^{129}\text{Xe}$ . The prominent features at about 4.7 Hz and 13 Hz correspond to the Larmor oscillation of the co-located  $^{129}\text{Xe}$  and  $^3\text{He}$  spins in one sample cell at an applied magnetic field of 400 nT inside BMSR-2. **c)** Free spin-precession signal of a polarized  $^3\text{He}$  sample cell, recorded by means of a low- $T_c$  SQUID gradiometer (sampling rate: 250 Hz). **d)** Envelope of the decaying signal amplitude. From an exponential fit to the data, a transverse relaxation time of  $T_2^* = (60.2 \pm 0.1) \text{ h}$  can be deduced.

$T_{1,\text{wall}}^{Xe}$  considerably and with it the measurement sensitivity of our  $^3\text{He}/^{129}\text{Xe}$  co-magnetometer are therefore essential.

### 3. Limit on Lorentz and CPT violation of the bound neutron using a free precession $^3\text{He}/^{129}\text{Xe}$ co-magnetometer

A great number of laboratory experiments has been designed to detect diminutive violations of Lorentz invariance. Among others, the Hughes-Drever-like experiments [14,15], have been performed to search for anomalous spin coupling to an anisotropy in space using electron and nuclear spins with steadily increasing sensitivity [16,17]. Lorentz violating theories should generally predict the existence of privileged reference systems. In contrast with the situation at the end of the 19th century, we have a rather unique choice nowadays for such a "preferred inertial frame", i.e., the frame where the Cosmic Microwave Background (CMB) looks isotropic. Trying to measure an anomalous coupling of spins to a relic background field which permeates the Universe and points in a preferred direction in spacetime as a sort of New Aether wind is a modern analogue of the original Michelson-Morley experiment. The theoretical framework presented by A. Kostelecky and colleagues parametrizes the general treatment of CPT- and Lorentz violating effects in a Standard Model extension (SME) [18].

To determine the leading-order effects of a Lorentz violating potential  $V$ , it suffices to use a non-relativistic description for the particles involved given by [1]

$$V = -\tilde{b}_J^w \cdot \sigma_J^w \quad (\text{with: } J = X, Y, Z; w = e, p, n). \quad (11)$$

Like in [19,20], we search for sidereal variations of the frequency of co-located spin species while the Earth and hence the laboratory reference frame rotates with respect to a relic background field. The observable to trace possible tiny sidereal frequency modulations is the combination of measured Larmor frequencies (see equation (5)) and the weighted phase differences, respectively. In March 2009, we performed a measurement consisting of 7 runs in series, each with a duration of 13 hours at least. The data of each run ( $j = 1, \dots, 7$ ) were divided into sequential time intervals  $i$  of length  $\tau = 3.2$  s ( $i = 1, \dots, N_j$ ). The number of obtained sub data-sets laid between  $14800 < N_j < 18000$  corresponding to observation times  $T_j$  of coherent spin-precessions in the range of  $13 \text{ h} < T_j < 16 \text{ h}$ . For each sub data-set a  $\chi^2$  minimization was performed, using the fit-function

$$A^i(t) = A_{He}^i \cdot \sin(\omega_{He}^i t) + B_{He}^i \cdot \cos(\omega_{He}^i t) + A_{Xe}^i \cdot \sin(\omega_{Xe}^i t) + B_{Xe}^i \cdot \cos(\omega_{Xe}^i t) + (c_0^i + c_{lin}^i \cdot t) \quad (12)$$

with a total of 8 fit-parameters. Within the relatively short time intervals, the term  $(c_0^i + c_{lin}^i \cdot t)$  presents the adequate parameterization of the SQUID offset showing a small linear drift due to the elevated  $1/f$ -noise at low frequencies (< 1 Hz) and some distinct distortions caused by mechanical vibrations [4]. For each sub data-set we finally obtain numbers for the respective fit parameters  $\omega_{He}^i, \omega_{Xe}^i, \varphi_{He}^i, \varphi_{Xe}^i$  including error bars. Thereby  $\varphi_{He}^i, \varphi_{Xe}^i$  are given by  $\varphi_{He(Xe)}^i = \arctan(B_{He(Xe)}^i / A_{He(Xe)}^i)$ . From these values the accumulated phases  $\Phi_{He(Xe)}^j(t)$  for each run  $j$  were determined and finally

$$\Delta\Phi^{(j)}(t) = \Phi_{He}^{(j)} - \gamma_{He} / \gamma_{Xe} \cdot \Phi_{Xe}^{(j)}. \quad (13)$$

Thus, one expects as a result a general phase offset  $\Delta\Phi^{(j)}(t) = \Phi^{(j)}_0 = \text{const.}$ , if no other drifts and noise sources come into play. Indeed, after subtraction of deterministic phase drifts like the linear phase shift  $\Phi_{\text{Earth}} = \Delta\omega_{\text{Earth}} \cdot t$  due to Earth's rotation, this results in phase residuals as shown in figure 2. Due to the exponential decay of the signal amplitudes, mainly that of Xenon with the much shorter  $T_2^*$  of only 4h to 5h, the *SNR* decreases resulting in an increase of the residual phase noise, i.e.,  $\sigma_{res} \sim \exp(t/T_{2,Xe}^*)$ . Non-magnetic spin interactions - if they exist - would be felt in a temporal change of the phase residuals. In the last step, a piecewise fit function was defined, which is a combined fit to all seven runs, now including the parametrization of the sidereal phase modulation

$$\Phi_{fit}^{SD}(t) = \sum_{j=1}^7 \Phi_{fit}^{(j)}(t) + \{a_s \cdot \sin(\Omega_{SD}(t - t_{0,1}) + \varphi_{SD}) - a_c \cdot \cos(\Omega_{SD}(t - t_{0,1}) + \varphi_{SD})\}. \quad (14)$$

$\Omega_{SD}$  is the angular frequency of the sidereal day and  $\varphi_{SD}$  represents the phase offset of the sidereal modulation at the local sidereal time  $t_{SD}=0.4053$  (units of sidereal day) at the beginning  $t_{0,1}$  of the first run with  $\varphi_{SD}=2\pi \cdot t_{SD}$ . From that, the RMS magnitude of the sidereal phase amplitude  $\Phi_{SD} = \sqrt{a_s^2 + a_c^2}$ , yielding  $(2.25 \pm 2.29)$  mrad (95% CL) could be extracted [21]. This result is consistent with no Lorentz- and CPT-violating effects. In terms of the SME [1] we can express  $\Phi_{SD}$  according to

$$\Phi_{SD} = \frac{2\pi}{\Omega_{SD}} \cdot \delta\nu_{\perp} \quad \text{with:} \quad 2\pi|\delta\nu_{\perp}| \cdot \hbar = \left| 2 \cdot (1 - \gamma_{He} / \gamma_{Xe}) \cdot \sin \chi \cdot \bar{b}_{\perp}^n \right| \quad (15)$$

$\chi$  is the angle between the Earth's rotation axis and the quantization axis of the spins ( $\chi=57^0$ ). Within the Schmidt model, the valence neutron of  $^3\text{He}$  and  $^{129}\text{Xe}$  determines the spin and the magnetic moment of the nucleus. Thus,  $^3\text{He}/^{129}\text{Xe}$  co-magnetometer is sensitive to the bound neutron parameter  $\tilde{b}_{\perp}^n$ .

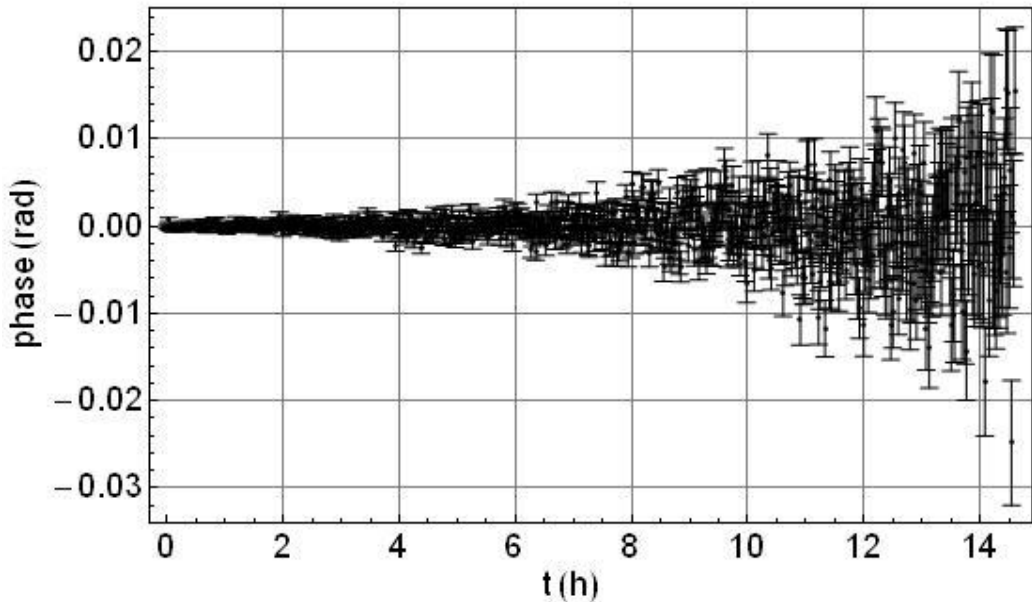


Figure 2: Phase residuals of the weighted phase difference  $\Delta\Phi$  (bandwidth:  $f_{BW} = 0.125$  Hz) after subtraction of deterministic phase drifts. The increase of the RMS of the phase noise with time is due to the exponential decay of the signal amplitudes, mainly that of Xenon.

With  $\tilde{b}_\perp^n < 3.7 \times 10^{-32}$  GeV (95% CL) we have set an upper limit on neutron spin coupling to possible Lorentz and CPT violating background tensor fields.

#### 4. Search for spin-dependent short range interaction of the bound neutron in ${}^3\text{He}/{}^{129}\text{Xe}$ clock comparison experiments

The existence of a new spin dependent short-range Yukawa force may be a signature of pseudoscalar boson particles like the "invisible axion" which is of interest as a possible component of cold dark matter. Originally, the axion was invented by Peccei and Quinn [22] to solve the so called "strong CP problem", i.e., presence of CP violating terms ( $\theta$ -term) in the QCD Lagrangian that arise from the non-trivial QCD vacuum structure. Such axions were not found in early searches, ruling out "standard axions" which have been related to the electroweak scale of symmetry breaking in the original Peccei-Quinn model. However, in case of a much higher energy breaking scale the axion becomes a very light, very weakly coupled and very long-lived particle that is named "invisible axion" [23]. Such hypothetical particle can mediate interaction between fermions which in case of monopole-dipole coupling violates parity  $P$  and time  $T$  symmetries. The Yukawa-type potential of this monopole-dipole interaction with range  $\lambda$  can be presented in the following form [2]:

$$V_{PS}(r) = \frac{\hbar^2}{8\pi m} g_s g_p (\sigma \cdot \hat{r}) \left( \frac{1}{\lambda r} + \frac{1}{r^2} \right) e^{-r/\lambda} \quad (16)$$

where  $g_s$  and  $g_p$  are dimensionless scalar and pseudo-scalar constants for the axion-fermion vertices,  $\hat{r}$  is the unit distance vector from the polarized  ${}^3\text{He}$ -nucleus to the unpolarized matter,  $m$  is the mass of nucleon,  $\sigma$  is the spin of the polarized nuclei, and  $\lambda$  is the range of the Yukawa force ( $\lambda = \hbar/m_a c \approx 20$  mm/  $m_a$  ( $\mu\text{eV}$ )).

Prior experiments and astronomical observations suggest that, if the axion exists, its mass  $m_a$  should lie within the "axion window"  $1\text{ }\mu\text{eV} < m_a < 1\text{ meV}$ , corresponding to a range  $0.2\text{ mm} < \lambda < 20\text{ mm}$ . The potential (equation (16)) effectively acts near the surface of a massive unpolarized sample ( $r \leq \lambda$ ) as a pseudomagnetic field and gives rise to a change in spin precession frequency  $\Delta\nu_{PS}$  with  $\Delta\nu_{PS} = V_\Sigma/h$ . The potential  $V_\Sigma$  is obtained by integration of  $V_{PS}(r)$  from equation (16) over the volume

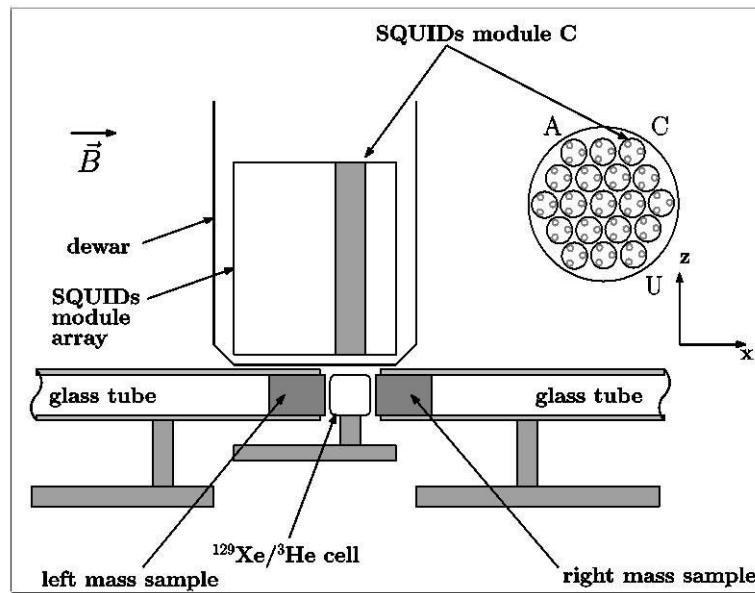


Figure 3: Sketch of the experimental setup inside BMSR-2

of the massive sample. Our cylindrical cell was made out of aluminosilicate glass (GE-180) with a diameter of 60 mm and a length of 60 mm. The spin-relaxation time (longitudinal wall relaxation time  $T_1$ ) of  $^3\text{He}$  was measured to be  $T_1 \approx 127$  h. The cell was filled outside BMSR-2 with a mixture of polarized  $^3\text{He}$  and  $^{129}\text{Xe}$  ( $\approx 2$  mbar and  $\approx 8$  mbar, respectively) and  $\text{N}_2$  ( $\approx 35$  mbar) used as buffer gas in order to suppress the Xenon relaxation due to van der Waals molecular coupling. After transportation into the inner shield, the cell was installed directly beneath the selected SQUIDs inside the Dewar. Two cylindrical glass tubes with a length of 1 m and an inner diameter of 60 mm were placed on a separate support with their axis along the axis of the cylindrical  $^3\text{He}/^{129}\text{Xe}$  sample cell. At their open ends towards the polarized sample cell, a test mass (Pb-glass) was installed. This is sketched in figure 3.

The tubes and with it the test mass could be moved horizontally from “close” position to “far away” position. At “close” position we had a minimum distance of 3 mm between the Pb-glass and the polarized gases. The glass tubes were installed in such a way that it was possible to move them without opening the door of the magnetic shielded room, i.e., without interruption of the  $^3\text{He}/^{129}\text{Xe}$  spin precession. Pb-glass cylinders (density 3.9 g/cm<sup>3</sup>) of diameter 57 mm and length 81 mm were used, since non-conducting materials prevented us from additional noises sources. If axion-fermion interaction exists, then it will cause a shift  $\pm v_{\text{PS}}$  in the combination of measured  $^3\text{He}/^{129}\text{Xe}$  Larmor frequencies (see equation (5)), respective phases. The sign depends on the direction of the normal vector on the surface of the front side of the Pb-glass cylinder relative to the direction of the holding magnetic field. Therefore, to look for an effect with the right signature, the measurement procedure was as follows: first, we measured the precession signals where only the left Pb-glass cylinder was installed. During the first time interval of 10800 sec, the Pb-glass cylinder was at “close” position. Then we continued with the Pb-glass sample at “far away” position for another  $\sim 30000$  sec. We repeated the same procedure, but now with the Pb-glass cylinder right to the  $^3\text{He}/^{129}\text{Xe}$  sample cell. To extract the precession frequencies we divided the data into sequential time intervals of 3.2s: For each time interval ( $i$ ) we applied the fit according to equation (12). In a similar way as discussed in section 2, the accumulated phases  $\Phi_{He(Xe)}^j(t)$  were determined for each particular positioning of the Pb-glass cylinder with respect to the  $^3\text{He}/^{129}\text{Xe}$  sample cell. In order to cancel the influence of ambient magnetic fields, we again build the weighted phase difference of the co-located precessing spin samples:  $\Delta\Phi = \Phi_{He} - \gamma_{He}/\gamma_{Xe} \cdot \Phi_{Xe}$ . Subtracting the deterministic phase drifts as described in [4,24], the effect we are looking for was sought as difference between linear terms ( $a_{lin} \cdot t$ ) of the residual phases measured with

**Table 1.** Results for  $v_{SP, left(right)}$  and  $\delta v$ .

Measurement	$v$ (nHz)	$\sigma_{corr}$ (nHz)	$\sigma_{stat}$ (nHz)
$v_{SP, left}$	46.6	11.1	1.4
$v_{SP, right}$	37.0	8.6	0.6
$\delta v$	4.8	7.0	0.5

Pb-glass sample at “close” and “far away” position:  $v_{SP, left(right)} = 1/2\pi \cdot (a_{lin, left(right)}^{close} - a_{lin, left(right)}^{far-away})$ .  
 Finally, we obtained the effect by combining the “left” and “right” Pb-glass measurements:

$$\delta v = 1/2 (v_{SP, left} - v_{SP, right}). \quad (17)$$

Results for  $v_{SP, left(right)}$  and  $\delta v$  are given in table 1. One can see that the “left” and “right” results within their error bars both give finite, positive values. This is obviously a constant frequency offset, since for the scalar-pseudoscalar coupling the sign should change.

The reasons are induced magnetic field gradients (paramagnetism) across the cell caused by the Pb-glass sample in its “close” position. With the weighted phase difference of the co-located sample spins, the Zeeman-term should drop out to first order. Taking into account the barometric formula, the center of gravity of the  $^3\text{He}$  and  $^{129}\text{Xe}$  gas in the sample cell is shifted by  $0.15 \mu\text{m}$ . This results in a field change of  $0.3 \text{ fT}$  at an induced field gradient of  $\approx 20 \text{ pT/cm}$ . With that one can easily explain the observed frequency offset. However, in the combination  $\delta v$  of the two measurements this effect drops out and we are left with a possible frequency shift, caused by a scalar-pseudoscalar short-range interaction. It is true, that only two measurements are not enough to check all the systematics in order to give a reasonable confidence level as an upper limit of the scalar-pseudoscalar coupling as a function of the axion mass. Nonetheless, our feasibility studies clearly demonstrate the high sensitivity and thus the high predictive power of investigating short-range interactions by using the free spin precession co-located  $^3\text{He}/^{129}\text{Xe}$  spin samples. In table 1 we also show correlated and uncorrelated errors obtained from the fit. Obviously the correlated error is much bigger than the uncorrelated one. This is understood from the fitting procedure we used to extract the linear terms from the residual phases. We use the correlated errors to set our sensitivity level for the dimensionless product  $g_{SP}$  in

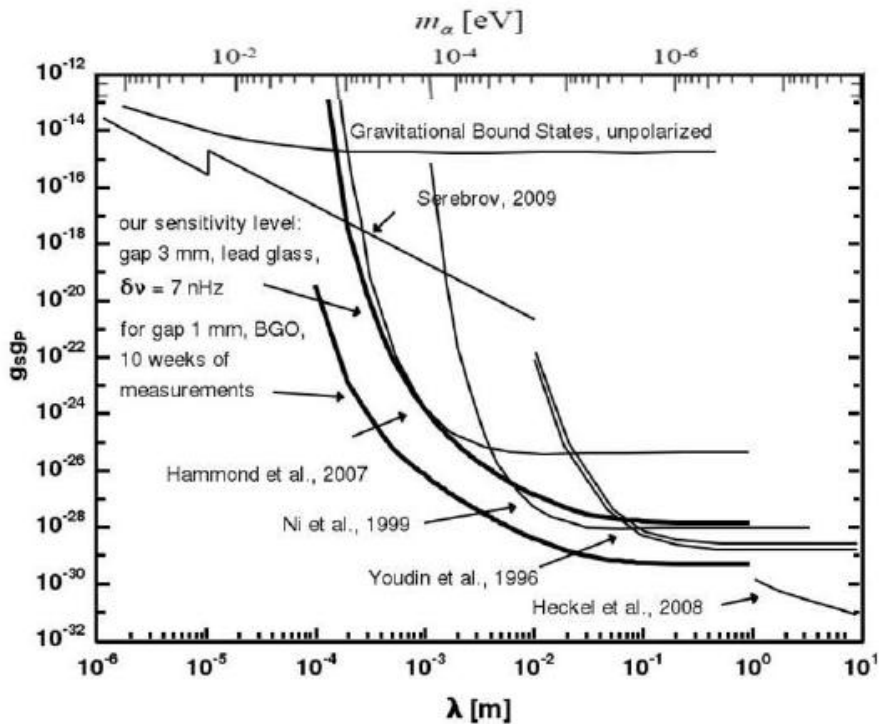


Figure 4: Exclusion plot for new spin dependent short-range forces [25]

the exclusion plot shown in figure 4 (thick black curve). This result follows from  $\bar{V}_\Sigma / h < \sigma_{corr}$ , where  $\bar{V}_\Sigma$  is sum of potentials (equation (16)) over the volume of the Pb-glass sample averaged over the  $^3\text{He}/^{129}\text{Xe}$  cell volume. Also shown (second thick curve in figure 4) is the exclusion level which we can achieve for longer measurement periods (10 weeks) using as unpolarized matter BGO crystals (almost twice more dense) and furthermore using a much smaller minimum distance between the polarized ( $^3\text{He}/^{129}\text{Xe}$ ) sample cell and the unpolarized BGO-crystal. The obtained statistical sensitivity level ( $\sigma_{stat}$ ) shown in table 1 also demonstrates that further progress can be achieved by suppression of the correlated error. Ways to do that are discussed in the appendix of [4].

## 5. Summary

$^3\text{He}/^{129}\text{Xe}$  clock-comparison experiments based on the detection of free spin precession of gaseous, nuclear polarized  $^3\text{He}$  and  $^{129}\text{Xe}$  samples with a SQUID as magnetic flux detector are particular attractive to investigate fundamental symmetries in nature. With the long nuclear spin coherence times obtained (in particular for  $^3\text{He}$ ), one gets sensitive to the nHz range in measuring tiny frequency shifts. There is room for improvements: efforts to increase  $T_2^*$  for  $^{129}\text{Xe}$  are essential to reach the pHz range.

## References

- [1] Kostelecký V A and Lane C D 1999 *Phys. Rev. D* **60** 116010
- [2] Moody J E and Wilczek F 1984 *Phys. Rev. D* **30** 130
- [3] Rosenberry M A and Chupp T E 2001 *Phys. Rev. Lett.* **86** 22
- [4] Gemmel C, Heil W, Karpuk S et al 2010 *Eur. Phys. Journal D* **57** 303-320
- [5] Kay S M 1993 *Fundamentals of Statistical Signal Processing: Estimation Theory* (Prentice Hall, New Jersey), Vol. 1.
- [6] Schmiedeskamp J, Heil W, Otten E W et al 2006 *Eur. Phys. Journal D* **38** 427-438
- [7] Deninger A, Heil W, Otten E W et al 2006 *Eur. Phys. Journal D* **38** 439-443
- [8] Schmiedeskamp J, Elmers H-J, Heil W et al 2006 *Eur. Phys. Journal D* **38** 445-454
- [9] Cates G D, Schaefer S R, Happer W, 1988 *Phys. Rev. A* **37** 2877
- [10] McGregor D D 1990 *Phys. Rev. A* **41** 2631
- [11] Bork J, Hahlbohm H-D, Klein R, Schnabel A, 2000 *Proc. Biomag* **2000** 970
- [12] Kilian W, 2001 Ph.D. thesis, Freie Universität Berlin, [www.diss.fu-berlin.de](http://www.diss.fu-berlin.de)
- [13] Schearer L D, Colegrove F D, Walters G K, 1963 *Phys. Rev. Lett.* **10** 108
- [14] Hughes V W, Robinson H G, and Beltran-Lopez V 1960 *Phys. Rev. Lett.* **4** 342
- [15] Drever R W P. 1961 *Philosophical Magazine*, **6** 683
- [16] Lamoreaux S K et al 1986 *Phys. Rev. Lett.* **57** 3125
- [17] Brown J M et al 2010 *Phys. Rev. Lett.* **105** 151604
- [18] Colladay D and Kostelecký V A 1998 *Phys. Rev. D* **58** 116002
- [19] Bear D et al 2000 *Phys. Rev. Lett.* **85** 5038
- [20] Bear D et al 2002 *Phys. Rev. Lett.* **89** 209902(E)
- [21] Gemmel C, Heil W, Karpuk S et al 2010 *Phys. Rev. D* **82** 111901
- [22] Peccei R D, Quinn H R 1977 *Phys. Rev. D* **16** 1791
- [23] Kim J E 1979 *Phys. Rev. Lett.* **43** 103; Shifman M A et al 1980 *Nucl. Phys. B* **166** 493-506
- [24] Burghoff M, Gemmel C, Heil W et al 2010 Proc. *Workshop on Experimental and Theoretical Approaches to Quantum States*
- [25] Heckel B R et al 2008 *Phys. Rev. D* **78** 092006; Youdin A N et al 1996 *Phys. Rev. Lett.* **77** 2170; Wei-Tou Ni et al 1999 *Phys. Rev. Lett.* **82** 2439; Hammond G D et al 2007 *Phys. Rev. Lett.* **98** 081101; Serebrov A P 2009 *arXiv:0902.1056*; Baessler S et al 2007 *Phys. Rev. D* **75** 075006